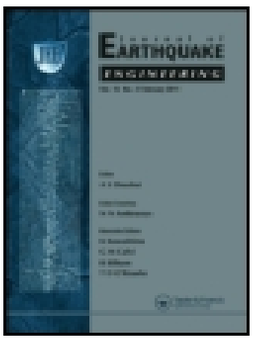

Journal of Earthquake Engineering

ISSN: 1363-2469 (Print) 1559-808X (Online) Journal homepage: http://www.tandfonline.com/loi/ueqe20

Seismic Vulnerability Assessment of a RC Pedestrian Crossing

Corneliu Cismaşiu, Filipe P. AmaranteDos Santos, Rui A. Da Silva Perdigão, Vasco M. S. Bernardo, Paulo X. Candeias, Alexandra R. Carvalho & Luís M. C. Guerreiro

To cite this article: Corneliu Cismaşiu, Filipe P. AmaranteDos Santos, Rui A. Da Silva Perdigão, Vasco M. S. Bernardo, Paulo X. Candeias, Alexandra R. Carvalho & Luís M. C. Guerreiro (2018): Seismic Vulnerability Assessment of a RC Pedestrian Crossing, Journal of Earthquake Engineering, DOI: 10.1080/13632469.2018.1453399

To link to this article: https://doi.org/10.1080/13632469.2018.1453399

Published online: 21 Mar 2018.

JOURNAL OF EARTHQUAKE ENGINEERING
https://doi.org/10.1080/13632469.2018.1453399

Taylor & Francis
Taylor & Francis Group

Seismic Vulnerability Assessment of a RC Pedestrian Crossing

Corneliu Cismaşiu[a], Filipe P. AmaranteDos Santos[a], Rui A. Da Silva Perdigão[b], Vasco M. S. Bernardo[b], Paulo X. Candeias[c], Alexandra R. Carvalho[c], and Luís M. C. Guerreiro[d]

[a]CERIS, ICIST and Faculdade de Ciências e Tecnologia, Universidade NOVA de Lisboa, Caparica, Portugal; [b]Faculdade de Ciências e Tecnologia, Universidade NOVA de Lisboa, Caparica, Portugal; [c]NESDE, Laboratório Nacional de Engenharia Civil, Lisboa, Portugal; [d]CERIS, ICIST and Instituto Superior Técnico, Universidade de Lisboa, Lisboa, Portugal

ABSTRACT

The paper addresses the seismic vulnerability assessment of a multi-span footbridge, prone to span unseating due to shorter seat lengths. The structure is representative of a series of pedestrian crossings located in the Southern part of Portugal, a region with a relevant seismicity. A probabilistic approach allows considering the variability of the seismic action and uncertainties in the definition of the material properties and/or structural behavior. Based on incremental dynamic analyses and corresponding fragility curves, it is shown that, for code compliance design acceleration, there is a significant probability that the structure will only suffer minor damage.

ARTICLE HISTORY
Received 24 November 2016
Accepted 2 January 2018

KEYWORDS
Rc Footbridges; Seismic Vulnerability Assessment; Operational Modal Analysis; Incremental Dynamic Analysis; Fragility Curves; Dowel Connection

1. Introduction

It is well known that the interruption of lifelines as a result of natural disasters can have major economic and social impacts, leading to much higher losses than the value of damage to the infrastructure itself. Therefore, although footbridges are not usually considered as critical lifeline structures, their collapse during an event such as an earthquake can be critical, as it might cause severe lifelines interruption. Despite new design strategies, like the ones contemplated in Eurocode 8, the Portuguese National Road Network includes many footbridges with high seismic vulnerability, susceptible to span unseating, due either to the lack of adequate seismic detailing, like short seats usually associated with older constructions, either to potential stronger shaking than the one considered in the original design.

In 2012, within the SUPERB research project [Cismasiu *et al.*, 2010], an experimental campaign has been launched, collecting relevant dynamic records of 16 footbridges located in the Southern part of Portugal, see Fig. 1a, a region with significant seismic activity.

Among them, as illustrated in Fig. 1b, several pedestrian crossings are located in a particularly sensitive area, close to the Faro airport and railway station, three hospitals, two fire departments, a large shopping center, a large university and several schools. The

CONTACT Corneliu Cismaşiu cornel@fct.unl.pt CERIS, ICIST and Faculdade de Ciências e Tecnologia, Universidade NOVA de Lisboa, Quinta da Torre, Caparica 2829-516, Portugal.

Color versions of one or more of the figures in the article can be found online at www.tandfonline.com/ueqe.

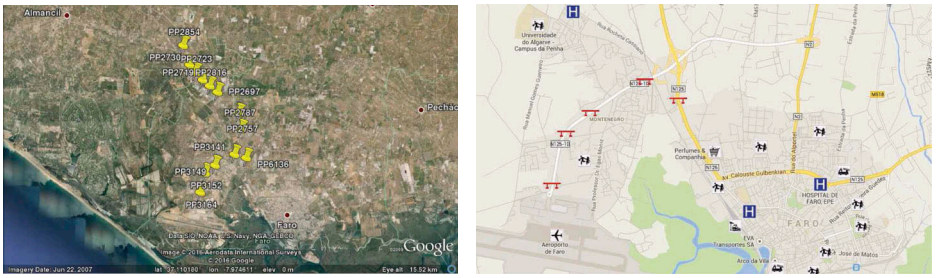

(a) Faro district (b) Particularly sensitive area

Figure 1. Location of the studied footbridges.

present study is focused on PP2787, a representative multi-span footbridge, prone to span unseating due to shorter seat lengths in the central spans.

Subsequent application of experimental modal identification techniques has enabled the accurate identification of the footbridge structural properties and to provide reliable data to support calibration, updating and validation of the corresponding numerical models.

These calibrated finite element (FE) numerical models were used to assess the seismic vulnerability of these structures employing a probabilistic approach that allows to consider the variability of the seismic action and uncertainties in the definition of the material properties and/or structural behavior.

2. Case Study: Footbridge PP2787

The pedestrian crossing PP2787 across the IC4 Portuguese highway in Faro district, see Fig. 2, is a simply supported RC footbridge, with three spans of 16.76, 24.7 and 16.76 m, and a vertical clearance of 5.4 m.

It is composed of two I-shaped prestressed girders with 1.20 m height, connected by a lower deck slab. The deck slab, which is built up of a 0.06 m precast slab and a cast-in-place concrete topping with 0.06 m, is supported by the bottom flanges of the main girders, as illustrated in Fig. 3a.

The connection of the main girders to the piers, see Fig. 3b, is materialized by a set of two steel dowels, with a diameter of 20 mm each, and an elastomeric bearing. The girders have vertical ducts in order to accommodate the dowels, which are filled with a non-retractable grout. The main piers, see Fig. 3c, are precast reinforced concrete elements, with a variable rectangular cross-section, ranging from 0.60×0.50 to 1.00×0.50 m^2, with superficial precast foundations. Note that, in the case of the two central piers, the 50 cm accounts for the seating length of two adjacent girders and the corresponding joint (see also Fig. 2d). If one also considers eventual assembling imperfections, it results in a relatively short seat length for each girder. The access to the bridges is materialized by a set of lateral precast reinforced concrete ramps and/or stairs, which are mainly built up of ribbed slabs supported by prestressed corbels, rigidly connected to the piers.

(a) Aerial view ©GoogleEarth (b) General view

(c) Access ramps (d) View of the seat in the central span

Figure 2. Pedestrian crossing PP2787 across the IC4 Portuguese highway.

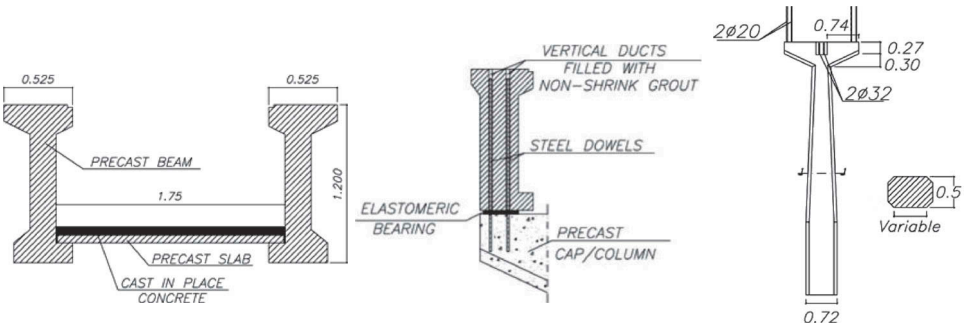

(a) Cross section of the deck (b) Deck-pier dowel connection (c) Main pier

Figure 3. Excerpts from the structural drawings of PP2787.

3. Ambient Modal Identification

The basic principles in experimental modal analysis and its evolution from input–output to output-only identification techniques have been presented by many authors, as for example [Ljung, 1999; Cunha and Caetano, 2006]. Nowadays, the output-only modal testing and identification is widespread and used for the dynamic characterization of Civil Engineering structures. Its main advantages and limitations are extensively discussed by Brincker and his co-workers in Brincker *et al.* [2000]. A literature review reveals many applications of output-only modal identification techniques to Civil Engineering

structures in general [Cunha and Caetano, 2006] and footbridges in particular [Galvin and Dominguez, 2005; Živanovic´ *et al.*, 2006; Benedettini and Gentile, 2008; Živanovic´ *et al.*, 2007].

During the ambient vibration tests (AVT), the velocity response was acquired using three MR2002-CE vibration monitoring systems from SYSCOM, each consisting of one MS2003+ triaxial velocity sensor and one vibration recorder, see Fig. 4.

The MR2002-CE is equipped with a digital signal processor to filter the signals coming from the sensor. To ensure synchronized data acquisition, the MR2002 clock is automatically updated using a GPS receiver. Preliminary FE models, developed based on the structural drawings, were used to provide estimates for the expected modal characteristics of the structure. These results were used to decide a data acquisition sampling-rate of 100 samples per second (the signal was cut-off at 80% of Nyquist frequency, allowing for the identification of frequencies as high as 40 Hz), the reference channel locations and the configurations of the roving sensors. As only three triaxial vibration monitoring systems were available, one was kept in the same location to guarantee three reference channels, while the remaining roving sensors were used in several setups to cover relevant grid points (located on the deck, on top of the piers and at 1/4, 1/2 and 3/4 of each span length). For each setup, ambient vibration data were acquired for 15 min.

Subsequent data processing using the Stochastic Subspace Identification (SSI-UPC) algorithm implemented in the operational modal analysis software ARTeMIS [Structural Vibration Solutions A/S, 2011a], allows to identify six stable modes (one longitudinal, three transverse and two vertical) with frequencies of 1.81, 1.95, 3.05, 4.04, 8.01 and 8.15 Hz, respectively, as illustrated in Fig. 5.

Figure 4. (a) SYSCOM MR2002-CE vibration monitoring system; (b) MS2003+ triaxial velocity sensor; (c) GPS antenna; (d) recorder.

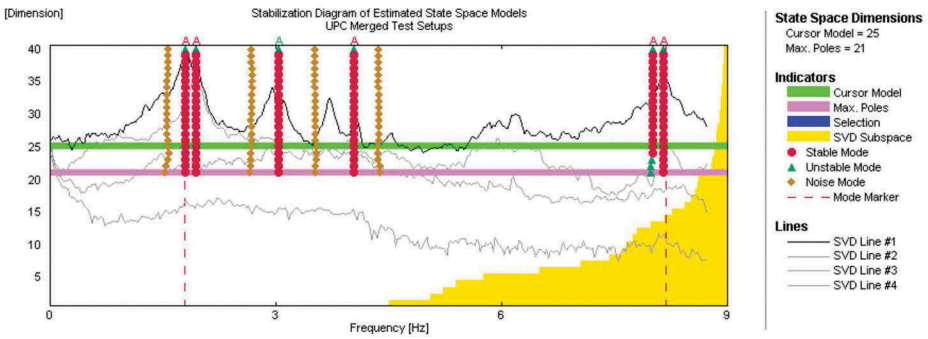

Figure 5. SSI-UPC: Stabilization diagram.

4. Experimental Characterization of the Dowel Connection

The PP2787 footbridge presents critical and potentially vulnerable connections between the main girders of the deck and the piers. To characterize its structural behavior when subjected to cyclic shear loads, a set of experimental tests were conducted in the facilities of the Earthquake Engineering and Structural Dynamics Division (NESDE) of the National Laboratory of Civil Engineering (LNEC).

As illustrated in Fig. 3b, a typical connection is built up of two 20 mm steel dowels and a neoprene bearing pad. Accordingly, a full scale prototype was built, designed to be representative of a typical footbridge connection. It consisted on a short girder supported on a reinforced concrete seating, with 10 mm thickness neoprene pads and the corresponding dowels. The reinforced concrete prototype was rigidly connected to the shake table using a steel supporting apparatus. The girders were actuated longitudinally by the table itself, using an additional steel strut which was fixed to a reaction wall. The scheme of the experimental setup and as some general views recorded during the tests are presented in Fig. 6a and b, respectively.

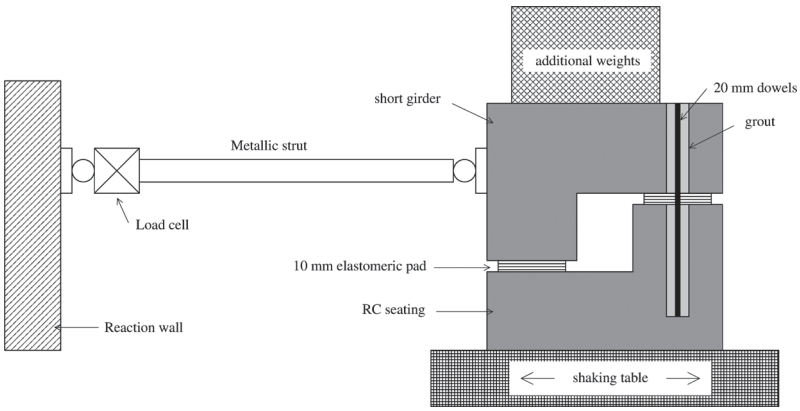

(a) Scheme of the experimental setup

(b) General views of the laboratory during testing

Figure 6. Setup for the experimental characterization of the dowel connection.

To understand and characterize the connection cumulative damage and the corresponding stiffness reduction, typical for earthquake scenarios, quasi-static cyclic displacements of growing amplitude were imposed to the prototype. The load time-history presented in Fig. 7a illustrates that the velocity of the imposed displacements was sufficiently low to prevent the occurrence of inertia forces and the associated dynamic effects.

The experimental structural response of the prototype connection is presented as the solid line in Fig. 7b. Analyzing the hysteretic cycles one can observe a degradation, both in terms of stiffness and strength, for increasing levels of displacement and with the number of imposed cycles. Regarding the damage observed during the experimental test, while the girder presented minor cracks, see Fig. 8a, the seating suffered a significant concrete failure as illustrated in Fig. 8b. During the tests, the dowels were essentially subjected to bending, with their failure occurring for a displacement of approximately 40 mm. One of the dowels has failed in two distinct places, associated with the formation of two plastic hinges, see Fig. 8c. The distance between these hinges was about 70 mm.

The results of the cyclic tests clearly illustrate the presence of cumulative damage in the connection, with evident consequences in the seismic structural vulnerability of the footbridge as a whole.

4.1. *FE Model*

While the AVT is known to be a very effective tool to identify the elastic modal properties of structures, the FE models to be used in their seismic vulnerability assessment must be able to simulate their nonlinear response as well.

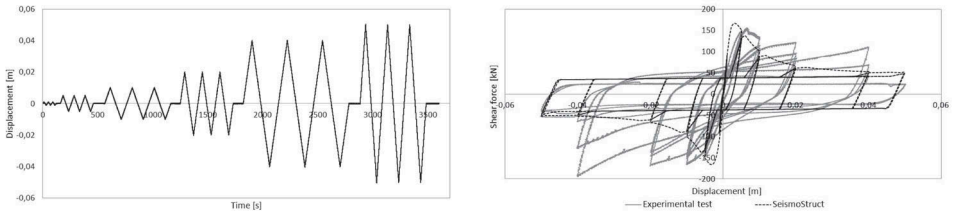

(a) Time-history of the imposed displacements (b) Force-displacement diagram

Figure 7. Cycling tests on the dowel connection.

(a) Minor cracks on the girder (b) Failure in the seating (c) Failure of the dowel

Figure 8. Damage observed after the experimental cyclic test.

In the case of the analyzed footbridge, its inelastic response to earthquakes is due, not only to the nonlinear response of the dowel connection, but also to the inelastic response of the piers. While results of the conducted experimental study can be used to calibrate the numerical model of the dowel connections between the main girders and the piers, no such experimental results were available for the piers. Therefore, their nonlinear behavior was taken into account in the FE model by inelastic constitutive material models for steel and concrete.

The numerical three-dimensional model of the PP2787 footbridge was developed with the commercial nonlinear FE code SeismoStruct [SeismoSoft, 2014] based on the design drawings. A computationally efficient uniaxial bilinear stress–strain model (stl_bl) with kinematic hardening, whereby the elastic range remains constant throughout the loading stages and the kinematic hardening rule for the yield surface is assumed as a linear function of the increment of plastic strain, was used to model the constitutive relationship of the rebars. In order to fully describe the mechanical characteristics of the steel, five calibrating parameters must be defined. These parameters, together with their adopted values to characterize the A500NR steel in the current FE model, are presented in Table 1.

The uniaxial nonlinear constant confinement model (con_ma) that follows the constitutive relationship proposed in Mander *et al.* [1988] and the cyclic rules proposed in Martinez-Rueda and Elnashai [1997] was used to model the constitutive relationship of the concrete. In this model, the confinement effects provided by the transverse reinforcement are incorporated through the rules given in Mander *et al.* [1988], whereby constant confining pressure is assumed throughout the entire stress–strain range. In order to fully describe the mechanical characteristics of the concrete, five calibrating parameters must be defined. These parameters, together with their adopted values to characterize the C35/45 (prestressed concrete elements) and C25/30 (other concrete elements) in the current FE model, are presented in Table 2. The effect of the pre-stressing cables was simulated using equivalent static forces.

The connections between the main girders of the deck and the piers were modeled through a specially designed combination of uniaxial RC cylindrical elements having a rosette configuration, see Fig. 9a. The cross-section of these elements and the corresponding material characteristics were calibrated to match the results of the experimental cyclic tests presented in Sec. 4. A general view of the complete FE model of the PP2787 pedestrian crossing in presented in Fig. 9b.

Table 1. Material characteristics of A500NR steel.

Modulus of elasticity (MPa)	2.0E5
Yield strength (MPa)	500
Strain hardening parameter (–)	0.005
Fracture/buckling strain (–)	0.1
Specific weight (kN/m^3)	78

Table 2. Material characteristics of concrete.

	C35/45		C25/30
Modulus of elasticity (MPa)	3.0E4		2.5E4
Mean compressive strength (MPa)	40.8		28.3
Mean tensile strength (MPa)		2.2	
Strain at peal stress (m/m)		0.002	
Specific weight (kN/m^3)		25	
Confinement factor		1.2	

(a) Rosette configuration (b) Three-dimensional global view

Figure 9. FE model of PP2787.

4.1.1. *FE Model Validation*

The validation of FE models is usually performed by comparing the numerical estimates with results obtained from experimental tests. In the present case, the validation of the PP2878 FE model was performed in two stages.

First, the quality of the numerical simulation of the dowel connection between the girders of the deck and the piers was investigated by reproducing the experimental cyclic tests presented in Sec. 4. When subjected to the same imposed displacements illustrated in Fig. 7a, the simulated force–displacement diagram, the dotted line in Fig. 7b, was in close agreement with the experimental curve, illustrated as the solid line in the same figure. Acceptable results were also observed in what respects the dissipated energy, see Fig. 10, with an average difference of 2.2% in the dissipated energy per cycle (55.49 kJ total experimental dissipated energy and 21.52 kJ cumulative difference between the experimental tests and the corresponding numerical simulation) and the same accumulated dissipated energy after the 18 hysteretic loops.

In the second stage, the results of a numerical modal analysis were compared with the outputs of the AVT presented in Sec. 3. The first five identified natural frequencies, see Fig. 5, and corresponding modes were used to calibrate the FE model. The coefficients of the Modal Assurance Criterion matrix and the values of the relative error in the frequencies, all presented in Fig. 11, illustrate a good corelation between the global modal characteristics of the real structure and the FE model. The corresponding modal configurations of the numerical model are given in Fig. 12.

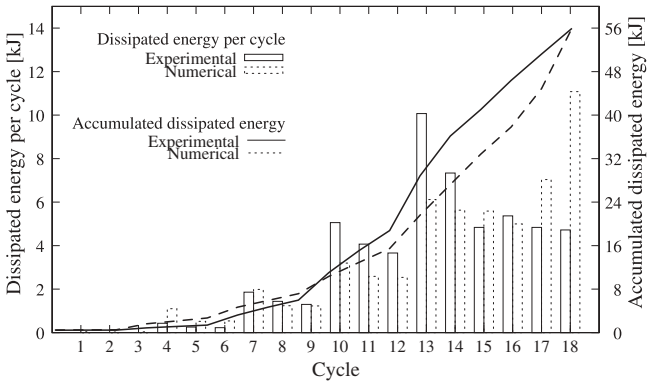

Figure 10. Dissipated energy in the dowel connection.

	Frequency	SeismoStruct					Error in
	[Hz]	1.79	2.00	3.10	4.08	7.94	frequency [%]
SSI-UPC	1.81	**0.9707**	0.0002	0.0020	0.0000	0.0039	1.10
	1.95	0.0002	**0.9183**	0.0012	0.0412	0.0004	2.56
	3.05	0.0015	0.0411	**0.6292**	0.0708	0.0932	1.64
	4.04	0.0077	0.0032	0.0004	**0.9726**	0.0004	0.99
	8.01	0.0097	0.0000	0.0002	0.0027	**0.9916**	0.87

Figure 11. Modal assurance criterion matrix.

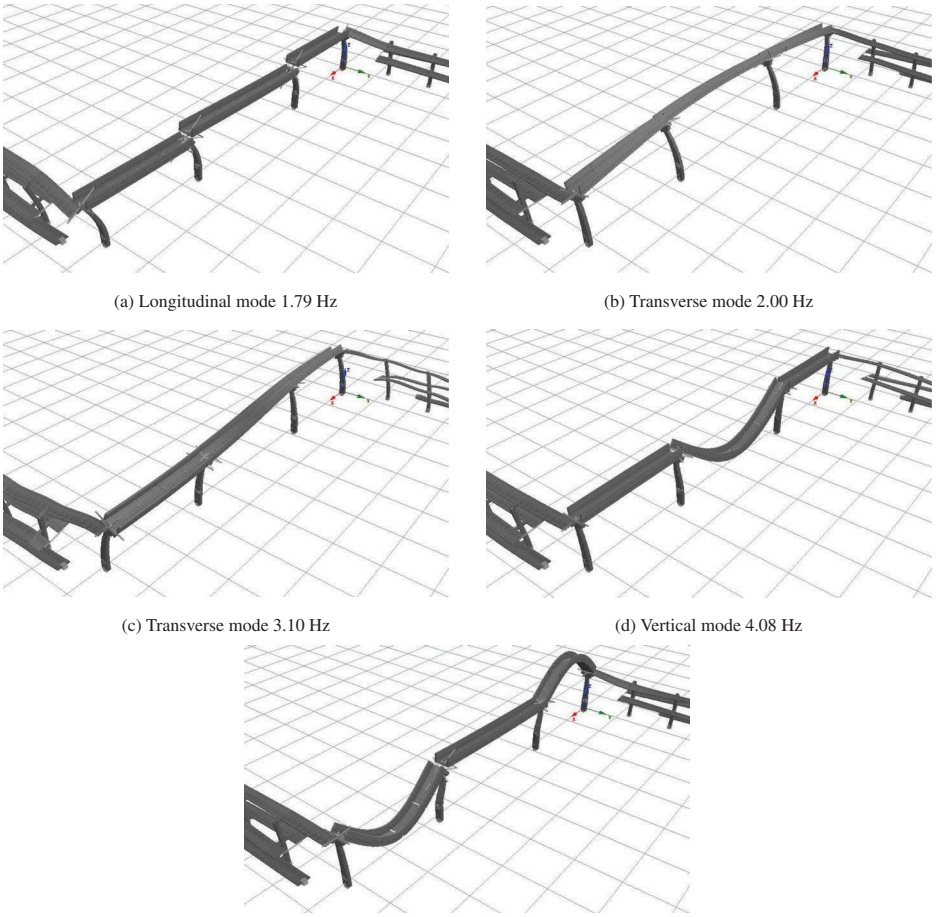

(a) Longitudinal mode 1.79 Hz

(b) Transverse mode 2.00 Hz

(c) Transverse mode 3.10 Hz

(d) Vertical mode 4.08 Hz

(e) Vertical mode 7.94 Hz

Figure 12. First vibration modes of the PP2787 FE model.

5. Seismic Vulnerability Assessment

In the last decade, a considerable amount of research has been published on the seismic vulnerability assessment of bridges, e.g. [Nielson and DesRoches, 2007], [Lee *et al.*, 2007], [Pottatheere and Renault, 2008], [Moschonas *et al.*, 2008], [Avşar *et al.*, 2011], [Avsar and

Yakut, 2012], [Seo and Linzell, 2012], [Kibboua *et al.*, 2014], [Siqueira *et al.*, 2012], [Choine *et al.*, 2015], [Djemai and Bensaibi, 2016], [Dezfuli and Alam, 2016], [Rogers and Seo, 2017]. An extended state-of-the-art review can be consulted in Billah and Alam [2015].

In the present work, a probabilistic approach was used to assess the seismic vulnerability of the PP2787 footbridge. This method allows to consider the variability of the seismic action and of several key parameters of the FE model using a statistical approach [Joint Committee on Structural Safety, 2001]. Subsequent incremental dynamic analyses (IDAs) allow to define several damage states (DSs) and to construct fragility curves that can be used to estimate the failure probability and the associated damage level for given peak ground accelerations (PGAs).

5.1. *Seismic Action*

To analyze the seismic vulnerability and the damage caused by earthquake loading, two distinct seismic scenarios associated to offshore source areas were considered in the present work, representing probable occurrences affecting the Faro region. The two scenarios are associated to the Marquês de Pombal Fault (MPF) and the Horseshoe Fault (HF), see Fig. 13, both located in the Atlantic Ocean at 100 and 140 km SW of the Portuguese coast (cape São Vicente), respectively, and historically associated to strong earthquakes.

The numerical simulation of the ground motion was performed using the RSSIM program [Carvalho *et al.*, 2008], developed at LNEC and based on the non-stationary stochastic method [Carvalho *et al.*, 2004] that takes into account finite fault effects. This

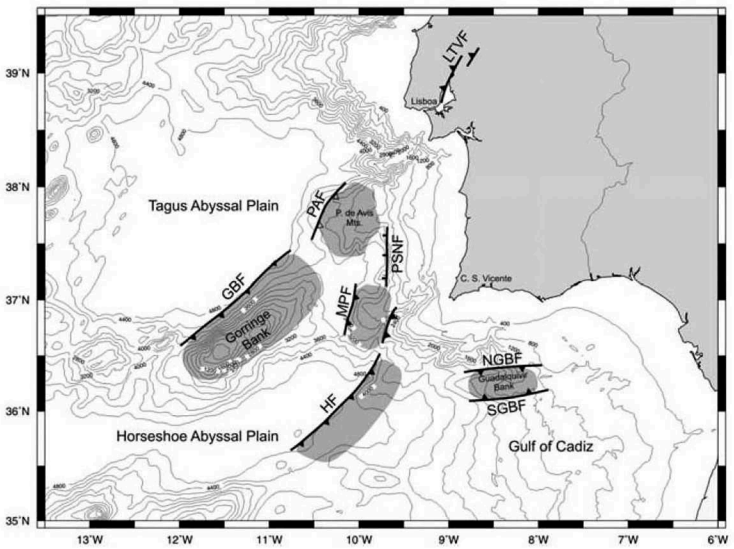

Figure 13. Major seismogenic zones in the SW of the Portuguese coast: GBF - Gorringe Bank Fault; PAF - Principes de Avis Fault; MPF - Marquês de Pombal Fault; HF - Horseshoe Fault; NGBF - Northern Guadalquivir Bank Fault; Southern Guadalquivir Bank Fault; PSNF - Pereira de Sousa Normal Fault; LTVF - Lower Tagus Valley Fault (adapted from Ribeiro *et al.*, 2009).

technique is particularly suitable for reproducing high frequency properties of the strong ground motion. The earthquakes were generated varying the rupture direction (NS, SN or random) along the faults extension and assuming magnitudes of M7.2 and M7.5 for the MPF and M7.8 for the HF, respectively. Using the generated earthquakes and combining different ground motions in two perpendicular directions, 100 seismic loading cases were set up, representing earthquakes with durations ranging from 20.57 to 94.64 s.

5.2. *Probabilistic Variability of Key Parameters*

To account for physical, mechanical and model uncertainties, the FE model was developed based on a certain number of key parameters whose values, according to Joint Committee on Structural Safety [2001], are assumed to have a probabilistic distribution. The chosen parameters, as well as their probabilistic characterization, are given in Table 3.

The parameter related to the age of the structure was considered in order to take into account potential corrosion of the dowels. According to ISO 9223 and EN ISO 12944-2, a C3 corrosive class must be considered for the Southern part of Portugal, yielding a corrosion velocity of 50 μm/year. Therefore, in the FE model, the cross-section of the dowels was accordingly reduced. The probabilistic distribution of the generated key parameters is given in Fig. 14, where the vertical dashed lines represent the values associated to the calibrated FE model presented in Sec. 4.1.1.

Using these parameters, 100 FE models of the footbridge were set up. From the previously generated load cases, randomly selected ground motions were associated to each model and subsequent IDAs were performed in order to construct the fragility curves and to assess the seismic vulnerability of the structure.

Table 3. Probabilistic characterization of key parameters.

Variable	Dist. type	Units	Mean	Std. deviation
C35/45 strength (deck)	Lognormal	MPa	40.8	4.48
C25/30 strength (others)	Lognormal	MPa	28.3	3.50
Concrete density	Normal	kN/m^3	25	0.75
Steel yield strength	Normal	MPa	500	30
Age of the structure	Normal	Years	16	5
Dowels model uncertainty	Lognormal	–	1	0.05

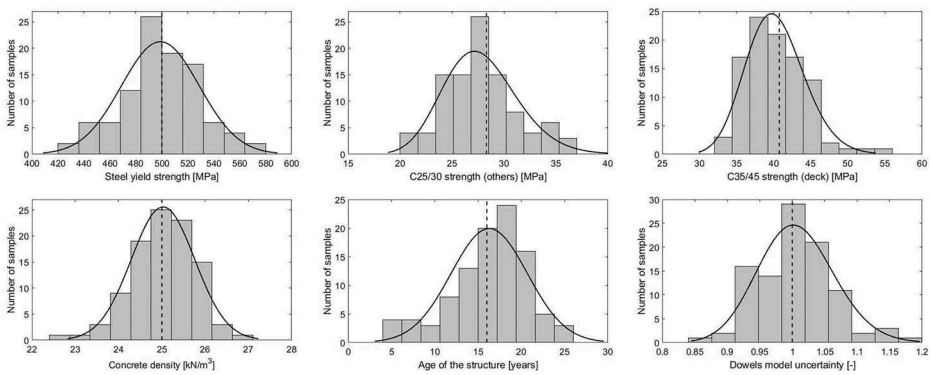

Figure 14. Probabilistic distribution of the chosen key parameters.

5.3. *Incremental Dynamic Analysis*

The IDA [Hamburger *et al.*, 2000; Vamvatsikos and Cornell, 2002] is a parametric method frequently used to estimate the structural seismic nonlinear response. To perform an IDA, the nonlinear numerical model of the structure is subjected to a series of ground motion time-histories of increasing intensity. In the present case, the PGA was incrementally scaled (eight steps) from a low elastic response value, 0.2 g, up to 1.6 g, value that guarantees the collapse in more than 50% of the FE models. The peak values of the base shear were then plotted against the corresponding deck horizontal displacement, for each of the runs, to yield the so-called dynamic pushover or IDA envelope curves. A total of 800 nonlinear analyses were performed to construct the 100 IDA envelope curves, see two examples in Fig. 15. These capacity curves were used next to define the damage states (DS_0 to DS_4) and to obtain the associated fragility curves.

5.4. *Damage States*

In the present work, the assessment of the structural damage was performed using five DS thresholds [Mouroux and Le Brun, 2006; HAZUS-MH, 2003]: DS_0 – none, DS_1 – slight, DS_2 – moderate, DS_3 – severe and DS_4 – extensive to collapse. As the piers and the structural connections were considered critical for the global behavior of the footbridge, two alternative definitions were used to define the DS thresholds, one for the piers and another one for the dowel connections. The definition of the DS thresholds for the piers was done according to Vargas *et al.* [2014], using the simplified bilinear form of the IDA envelope curves, as a function of the yielding (d_y) and ultimate (d_u) displacements, as indicated in Table 4. A qualitative description of the defined DSs is given in Table 5.

In what respects the dowels, their DS thresholds were based on the experimental results reported in Sec. 4 and illustrated in Fig. 16.

The values indicated in Table 4 related to the deck/pier connection correspond to the elastic limit of the dowels (DS1), relative displacement associated to a 20% loss in the maximum force transmitted by the connection (DS2), failure of the dowels (DS3) and deck unseating (DS4).

The DS thresholds for the piers, established for all the IDA envelope curves, are represented in Fig. 17, where one can see that their dispersion increases with the DSs indicating that uncertainties, at a certain level of damage, increase with the nonlinearity of the response.

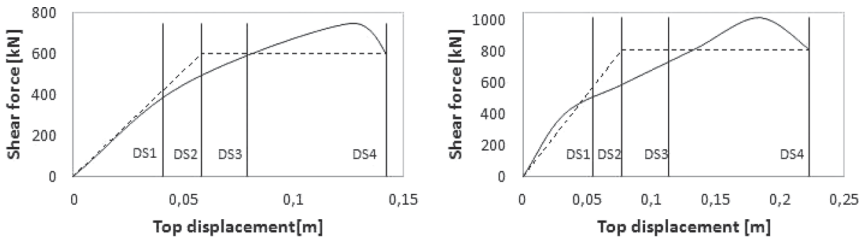

(a) Longitudinal direction (b) Transverse direction

Figure 15. Examples of IDA envelop curves and their bi-linearization.

Table 4. Definition of the DS thresholds.

Damage in the piers (deck absolute IDA displacement)	Damage in the connection (deck/pier relative IDA displacement) [m]
$DS_1 = 0.7\ d_y$	0.003
$DS_2 = d_y$	0.0065
$DS_3 = DS_2 + 0.25\ (d_u - d_y)$	0.0400
$DS_4 = d_u$	0.1950

Table 5. Qualitative description of the DSs.

Damage state	Description
DS0 (None)	No damage or evidence of new cracking
DS1 (Slight)	Slightly opening of preexisting cracks. New minor cracks starting to develop at the bottom of the piers and in the grout around the dowels. The structure response is mainly elastic.
DS2 (Moderate)	Cracking damage throughout the piers and in the grout around the dowels. Local detachment of the concrete cover in the sitting areas. Yielding of the dowels and crushing of the grout and concrete in the connection area, with an associated reduction of the load-bearing capacity.
DS3 (Severe)	Extensive cracking of the concrete and formation of plastic hinges at the bottom of the piers. Complete failure of the dowels.
DS4 (Extensive to collapse)	Imminent collapse or collapse of the structure due either to deck unseating or to the complete failure of the piers.

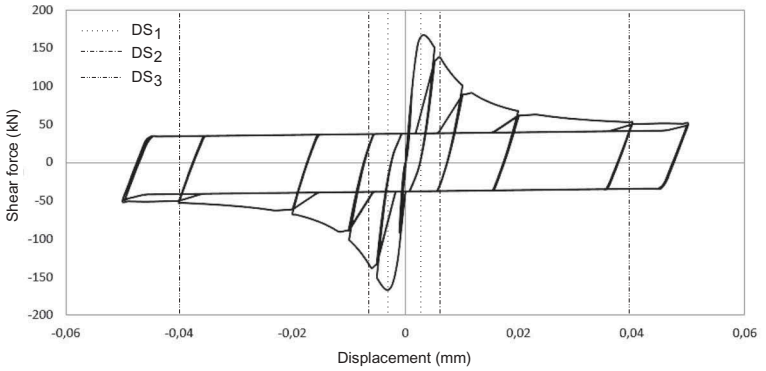

Figure 16. DSs thresholds for the dowells unseating.

5.5. *Fragility Curves*

For each DS threshold, the corresponding fragility curve gives the probability that the actual seismic demand of the footbridge as a whole, or of one of its components, exceeds the corresponding threshold, representative of a given performance level of interest [Nielson and DesRoches, 2007]. Each fragility curve, assumed to follow a standard log-normal cumulative distribution function φ, is defined in Eq. (1),

$$P[\mathrm{DS}_i/d] = \phi\left[\frac{1}{\beta_{\mathrm{DS}_i}}\mathrm{In}\left(\frac{d}{\mathrm{DS}_i}\right)\right] \tag{1}$$

where d is the IDA displacement and β_{DSi} the standard deviation of the natural logarithm of variable DS_i. The resulting global fragility curves, expressed as a function of PGA and observing both the nonlinear behavior of the piers and dowel connections, are given in Fig. 18. To assess the seismic vulnerability of the structure, in the same figure are

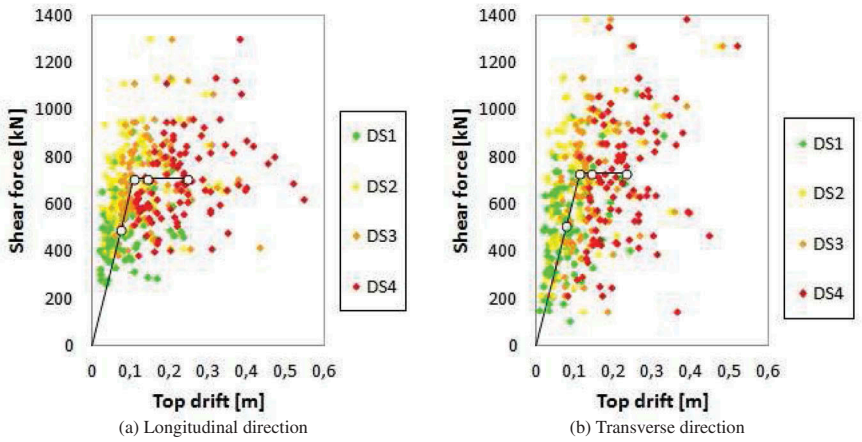

Figure 17. DSs thresholds for the piers for all performed analyses.

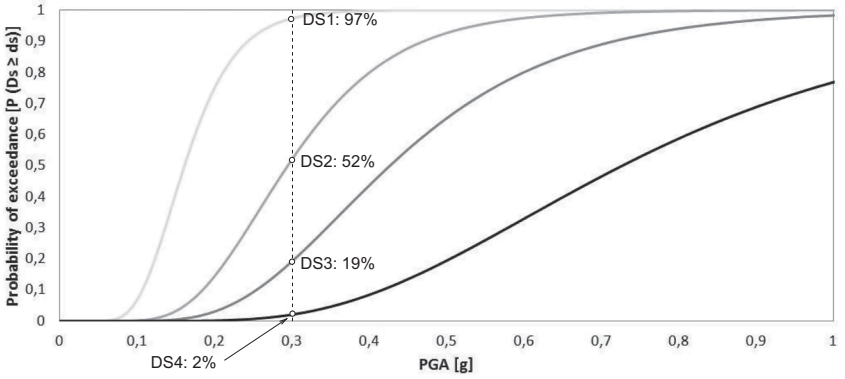

Figure 18. Global fragility curves of PP2787 footbridge.

emphasized the probabilities of exceeding the DS thresholds for a design PGA of 0.3 g, typical for the region where the footbridge is located.

Analyzing Fig. 18 one can readily see that, for a code compliance design acceleration, although there is a significative (97%) probability that the structure will suffer damage, it will only suffer minor (45%) to moderate (33%) damage.

A closer inspection of the results, see Fig. 19, reveals that the probability of occurrence of at least slight damage is similar for the dowels (83%) and piers (78%). However, there is a relatively small probability (26%) of moderate damage in the dowels. Therefore, a retrofit of the dowel connections is not justified, not only because of their probable low level of damage during an earthquake but also because, for larger PGA, the global damage of the structure is caused mainly by the nonlinear behavior of the piers.

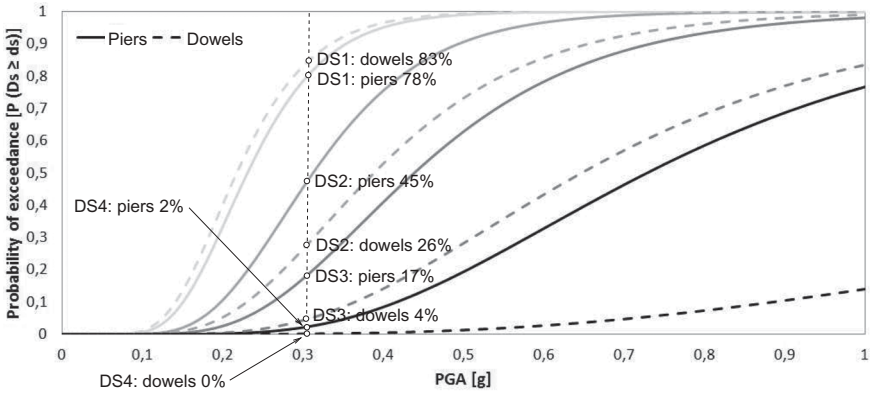

Figure 19. Fragility curves for dowels and piers conclusions.

6. Conclusions

The seismic vulnerability assessment of a multi-span footbridge, PP2787, representative of a series of pedestrian crossings located in the Southern part of Portugal, was successfully performed in the present work.

Relevant dynamic records collected during an ambient vibration modal identification campaign, were used to identify the footbridge structural properties and to provide reliable data to support calibration, updating and validation of the corresponding numerical models.

Next, the structural behavior of the critical and potential vulnerable dowel connection between the main girders of the deck and the piers was characterized by a set of experimental tests conducted in the facilities of NESDE at LNEC, providing important data for the calibration of the nonlinear numerical model of these connections.

Validation of the PP2787 FE numerical model was successfully performed, both in terms of modal characteristics and nonlinear behavior of the dowel connections.

A probabilistic approach that allows to consider the variability of the seismic action and uncertainties in the definition of several material properties and/or structural behavior was used in combination with IDAs in order to define DS thresholds and corresponding fragility curves.

Subsequent analysis of the fragility curves allows to conclude that the footbridge is expected to sustain, undamaged, the seismic loads associated to a 0.1g PGA earthquake. For increasing PGAs (0.1 to 0.2 g), the expected damage is mainly slight, evenly distributed between the piers and their dowel connections to the main girders. A significant change in the damage distribution is observed for increasing PGAs, as the piers start showing higher damage levels than the dowel connections. As an example, for 0.3 g one can readily see that, while there is a significant probability (45%) of moderate to severe (17%) damage in the piers, the probability of moderate to severe damage in the dowel connection is much lower (26% and 4%, respectively). One recalls here that the complete failure of the dowels is only associated to severe damage, as it does not imply the collapse of the footbridge. The piers appear to be the critical structural elements of the footbridge, as the probability of their of collapse is always higher than the probability of deck unseating.

One may conclude that, for a code compliance design acceleration, there is a significant probability that the structure will only suffer minor to moderate damage. Therefore, the seismic vulnerability of the structure is low and a retrofit of the dowel connections seems to be not justified.

Acknowledgments

Cooperation with Doctor Alfredo Campos Costa, head of the Earthquake Engineering and Structural Dynamics Division of the National Laboratory of Civil Engineering and Engineers Carlos F. S. Pimentel and Tiago M. M. Rodrigues, the former and the actual head of the Special Structures Division of *Infraestruturas de Portugal*, is gratefully acknowledged.

Funding

This work was supported by contract PTDC/ECM/117618/2010 with *Fundação para a Ciência e Tecnologia*.

References

Avşar, Ö., Yakut, A. and Caner, A. [2011] "Analytical fragility curves for ordinary highway bridges in Turkey," *Earthquake Spectra* **27**(4), 971–996. doi:10.1193/1.3651349

Avsar, O. and Yakut, A. [2012] "Seismic vulnerability assessment criteria for RC ordinary highway bridges in Turkey," *Structural Engineering and Mechanics* **43**(1), 127–145. doi:10.12989/sem.2012.43.1.127

Benedettini, F. and Gentile, C. [2008, February 4–7]. "FE modelling of a cable-stayed bridge based on operational modal analysis," *Proc. of theIMAC XXVI: A Conference & Exposition on Structural Dynamics,*Orlando, Florida USA.

Billah, A. H. M. M. and Alam, M. S. [2015] "Seismic fragility assessment of highway bridges: a state-of-the-art review," *Structure and Infrastructure Engineering* **11**(6), 804–832. doi:10.1080/15732479.2014.912243

Brincker, R., Zhang, L. and Andersen, P. [2000] "Output-only modal analysis by frequency domain decomposition," *ISMA25: International Conference on Noise and Vibration Engineering* **2**, 717–723.

Carvalho, A., Campos Costa, A. and Sousa Oliveira, C. [2004]. "A stochastic finite fault modeling for the 1755 Lisbon earthquake," *13WCEE: World Conference on Earth-Quake Engineering*, Vancouver, BC. Paper no. 2194.

Carvalho, A., Zonno, G., Franceschina, G., Bilé Serra, J. and Campos Costa, A. [2008] "Earthquake shaking scenarios for the metropolitan area of Lisbon," *Soil Dynamics and Earthquake Engineering* **28**, 347–364. doi:10.1016/j.soildyn.2007.07.009

Choine, M. N., O'Connor, A. J. and Padgett, J. E. [2015] "Comparison between the seismic performance of integral and jointed concrete bridges," *Journal of Earthquake Engineering* **19**(1), 172–191. doi:10.1080/13632469.2014.946163

Cismasiu, C., Santos, F. P. A., Costa, A. C., Candeias, P. and Guerreiro, L. [2010]. "PTDC/ECM/117618/2010 - Seismic unseating prevention elements for retrofitting of bridges," Technical report, Fundação para a Ciência e a Tecnologia, Ministério da Edu- cação e Ciência, Portugal.

Cunha, A. and Caetano, E. [2006] "Experimental modal analysis of Civil Engineering structures," *Sound and Vibration* **40**(6), 12–20.

Dezfuli, F. H. and Alam, M. S. [2016] "Seismic vulnerability assessment of a steel-girder highway bridge equipped with different SMA wire-based smart elastomeric isolators," *Smart Materials and Structures* **25**(7), 16. doi:10.1088/0964-1726/25/7/075039

Djemai, M. C. and Bensaibi, M. [2016]. "Seismic vulnerability assessment of Tipaza bridges," *3rd International Conference on Information and Communication Technologies for Disaster Management (ICT-DM)*, Vienna, Austria. p. 3.

Galvin, P. and Dominguez, J. [2005, January 31–February 3]. "Modal identification of a pedestrian bridge by output- only analysis," *Proc. of IMAC-XXIII: A conference & Exposition on Structural Dynamics,*Orlando, Florida, USA.

Hamburger, R. O., Foutch, D. A. and Cornell, C. A. [2000]. "Performance basis of guidelines for evaluation, upgrade and design of moment-resisting steel frames," *12WCEE: World Conference on Earthquake Engineering*, Auckland, New Zealand. paper No. 2543.

HAZUS-MH. [2003]. *Multi-hazard loss estimation methodology: earthquake model. FEMA* (available online at http://www.fema.gov/hazus).

Joint Committee on Structural Safety. [2001]. *JCSS probabilistic model code*. (online) (available online at http://www.jcss.byg.dtu.dk).

Kibboua, A., Bechtoula, H., Mehani, Y. and Naili, M. [2014] "Vulnerability assessment of reinforced concrete bridge structures in Algiers using scenario earthquakes," *Bulletin of Earthquake Engineering* **12**(2), 807–827. doi:10.1007/s10518-013-9523-7

Lee, S. M., Kim, T. J. and Kang, S. L. [2007] "Development of fragility curves for bridges in Korea," *KSCE Journal of Civil Engineering* **11**(3), 165–174. doi:10.1007/BF02823897

Ljung, L. [1999] *System Identification: Theory for the User*, Prentice Hall, 2nd edition.

Mander, J. B., Priestley, M. J. N. and Park, R. [1988] "Theoretical stress-strain model for confined concrete," *Journal of Structural Engineering* **114**(8), 1804–1826. doi:10.1061/(ASCE)0733-9445(1988)114:8(1804)

Martinez-Rueda, J. E. and Elnashai, A. S. [1997] "Confined concrete model under cyclic load," *Materials and Structures* **30**(197), 139–147. doi:10.1007/BF02486385

Moschonas, I. F., Kappos, A. J., Panetsos, P., Papadopoulos, V., Makarios, T. and Thanopoulos, P. [2008] "Seismic fragility curves for Greek bridges: methodology and case studies," *Bulletin of Earthquake Engineering* **7**(2), 439–468. doi:10.1007/s10518-008-9077-2

Mouroux, P. and Le Brun, B. [2006] *RISK-UE Project: An Advanced Approach to Earth- Quake Risk Scenarios with Application to Different European Towns*, Springer Netherlands, Dordrecht. 479–508.

Nielson, B. G. and DesRoches, R. [2007] "Analytical seismic fragility curves for typical bridges in the central and southeastern United States," *Earthquake Spectra* **23**(3), 615–633. doi:10.1193/1.2756815

Pottatheere, P. and Renault, P. [2008]. "Seismic vulnerability assessment of skew bridges," *14WCEE: World Conference on Earthquake Engineering*, Beijing, China. p. 12. Retrieved from http://www.14wcee.org/Proceedings/files/06-0061.PDF

Ribeiro, A., Mendes-Victor, L., Matias, L., Terrinha, P., Cabral, J., and Zitellini, N. [2009] "The 1755 Lisbon Earthquake: A Review and the Proposal for a Tsunami Early Warning System in the Gulf of Cadiz," in *The 1755 lisbon earthquake: revisited. Geotechnical, Geological, and Earthquake Engineering* (Springer, Dordrecht), Vol. 7. doi:10.1007/978-1-4020-8609-0_26

Rogers, L. P. and Seo, J. [2017] "Vulnerability sensitivity of curved precast-concrete I-girder bridges with various configurations subjected to multiple ground motions," *Journal of Bridge Engineering* **22**(2), 04016118. doi:10.1061/(ASCE)BE.1943-5592.0000973

SeismoSoft. [2014]. *SeismoStruct: A Computer Program for Static and Dynamic Nonlinear Analysis of Framed Structures* (available online at http://www.seismosoft.com).

Seo, J. and Linzell, D. G. [2012] "Horizontally curved steel bridge seismic vulnerability assessment," *Engineering Structures* **34**, 21–32. doi:10.1016/j.engstruct.2011.09.008

Siqueira, G. H., Sanda, A. S., Paultre, P. and Padgett, J. E. [2012] "Fragility curves for isolated bridges in eastern Canada using experimental results," *Engineering Structures* **74**, 311–324. doi:10.1016/j.engstruct.2014.04.053

Structural Vibration Solutions A/S. [2011a]. "*ARTeMIS extractor Pro*. NOVI Science Park, Niels Jernes Vej 10, DK-9220," Aalborg East, Denmark. Release 5.3.

Vamvatsikos, D. and Cornell, C. [2002] "Incremental dynamic analysis," *Earthquake Engineering and Structural Dynamics* **31**, 491–514.

Vargas, Y. F., Barbat, A. H., Pujades, L. G. and Hurtado, J. E. [2014] "Probabilistic seismic risk evaluation of reinforced concrete buildings," *Proceedings of the Institution of Civil Engineers - Structures and Buildings* **167**(6), 327–336. doi:10.1680/stbu.12.00031

Živanovic´, S., Pavic, A. and Reynolds, P. [2006] "Modal testing and FE model tuning of a lively footbridge structure," *Engineering Structures* **28**(6), 857–868. doi:10.1016/j.engstruct.2005.10.012

Živanovic´, S., Pavic, A. and Reynolds, P. [2007] "Finite element modelling and updating of a lively footbridge: the complete process," *Journal of Sound and Vibration* **301**(1), 126–145. doi:10.1016/j.jsv.2006.09.024